Marine Structures 101 (2025) 103759

Contents lists available at ScienceDirect

Marine Structures

journal homepage: www.elsevier.com/locate/marstruc

Research paper

PSO-based design and optimization of jacket substructures for offshore wind turbines

Borja Benítez-Suárez *, Román Quevedo-Reina, Guillermo M. Álamo, Luis A. Padrón

Instituto Universitario de Sistemas Inteligentes y Aplicaciones Numéricas en Ingeniería (SIANI), Universidad de Las Palmas de Gran Canaria (ULPGC), Edif. Central del Parque Científico-Tecnológico, Campus Universitario de Tafira, Las Palmas de Gran Canaria, 35017, Spain

ARTICLE INFO

Keywords:
Wind energy
Offshore wind turbine
Jacket support structure
Structural optimization
Particle swarm optimization
Finite element analysis

ABSTRACT

The search for more and better wind resources pushes offshore wind farms further into deeper waters, where jacket support structures become a competitive alternative to monopiles for bottom-fixed offshore wind turbines. In this context, this paper proposes a cost-effective methodology for the autonomous design that facilitates the generation of preliminary candidate designs of jacket substructures, reaching a level of detail suitable for the initial design phase. A Particle Swarm Optimization algorithm, with precomputed initial swarms, is used as a search and optimization tool. The proposed strategy is able to find candidate designs that satisfy, with a minimum use of material, a wide range of Ultimate Limit States, Fatigue Limit States and Geometrical Restrictions. It is shown that the use of a precomputed initial swarm generated taking into account a starting concept design of the structures with a low computational cost, instead of a standard random population, significantly improves the efficacy and efficiency of the algorithm. A reference case, based on the NREL-5MW wind turbine and its OC4 reference jacket support structure, is used for studying and illustrating the capabilities of the proposal.

1. Introduction

Climate change is one of the greatest challenges that humanity is facing in this 21st century. To address this threat, it is necessary to encourage an energy transition involving a series of transformations in the patterns of energy production, distribution, and consumption to increase sustainability. The geopolitical risks currently being experienced in the world, especially in Europe [1], are also encouraging the development and spread of renewable energies.

One of the most promising renewable energy sources is offshore wind energy. A total of 57.2 GW are currently installed worldwide, with China representing the largest producer of electricity through Offshore Wind Turbines (OWTs) with 48% of the global installed capacity. A further 90 GW are expected to be added until 2026 [2]. Wind farms at sea have several advantages over those on land. They avoid noise pollution, reduce visual impact, and preserve land spaces. Moreover, they benefit from better wind resources at sea, where the wind speed is higher, the obstacles are fewer, and the direction is more stable. As OWT move further away from the coast, wind conditions improve (wind speed principally) and the negative impacts on humans are reduced. At the same time, as depths increase, monopiles start to lose their competitive advantages [3,4] and jacket-type support structures start to gain interest (until depth becomes so high that floating wind turbines become the only option).

* Corresponding author.
E-mail address: borja.benitez@ulpgc.es (B. Benítez-Suárez).

https://doi.org/10.1016/j.marstruc.2024.103759
Received 18 April 2024; Received in revised form 11 November 2024; Accepted 7 December 2024

Available online 18 December 2024

The cost of substructure and foundations represents between 12% and 20% of the total investment in OWT projects, as noted by Johnston et al. [5] and GWEC [2]. A reduction of the cost in this section of the budget results in considerable project savings and increased operating profit.

Investigations in wind energy have been increasing significantly during the last decades (see, e.g., [6–8] for recent reviews). One of the points that the scientific community has focused on in recent years is proposing optimization methodologies. There are two approaches to proceed with optimization: gradient-based and gradient-free (heuristics) methods. Both have been used as optimization methodologies for OWTs, their substructures, and foundations. For example, Chew et al. [9] proposed an analytical gradient-based methodology to reduce the mass of the jacket by focusing on its bars (legs and braces), while considering sizing based on eigenfrequency, extreme loads, and fatigue loads. In other article, Chew et al. [10] proposed a gradient-based optimization algorithm that evaluates the objective function analytically. A global optimum solution was achieved using a multi-star strategy with all design solutions converging, with and without joint cans. They conclude that considering many constraints can make the optimization algorithm more likely to find a global optimum. Both buckling and fatigue constraints significantly influenced the design. Oest et al. [11] proposed three optimization approaches based on damage equivalent loads and quasi-static analysis. Also, some dynamic phenomena were considered: the natural frequency and fatigue checks. Marjan and Huang [12] propose a Topological Optimization to optimize jackets against their fatigue strength and material utilization factor, combined with ANSYS and DNV Sesam for structural verifications. The OC4 reference jacket [13] is employed as reference substructure in these papers [9–12] as support structure of the NREL 5-MW turbine [14]. Sandal et al. [15] proposed a gradient-based methodology for optimizing substructures, which are then used as initial models for financial studies. A Finite Element Model (FEM) was used to evaluate Fatigue and Ultimate Limit State constraints. It was also analyzed how the jacket mass optimization depends on the amount of bracing and on the leg lengths. In view of the increasing size of the OWT, the methodology was validated with the 10-MW OWT [16]. In another paper, Sandal et al. [17] presented an optimization methodology based on the Interior Point OPTimizer algorithms to optimize jackets and foundations (piles and suction caissons) in clay and sandy soils.

Heuristic methods are based on the behavior of nature and its inhabitants. Gentils et al. [18] used Genetic Algorithms (GA) as an optimization tool for monopile substructures, taking fatigue and natural frequency as design drivers. Zheng et al. [19] used GA combined with a structural surrogate model to generate optimized pre-designs of jackets that meet the constraints. Wang et al. [20] used GA together with a FEM to optimize the jacket mass, emphasizing the modal analysis and the strength capacity of the joints as a function of their geometry, Y-type, K-type and X-type. Oliveira Cruz et al. [21] combined several optimization algorithms: GE, Differential Evolution, Tournament Selection Method, Multiple Constraint Ranking, Adaptive Penalty Method, and Helper-and-Equivalent Optimization to optimize the mass of the jacket. The design variables considered were diameters and thicknesses. The constraints taken into account were related to the natural frequency of the system and the Ultimate Limit State criteria. Other studies have focused on improving the design of other specific subsystems of the OWT. For instance, Yeon-Seung et al. [22] used a heuristic trial-and-error approach to successfully reduce weight and minimize stress in the transition piece. Ali et al. [23] focused on optimizing the OWT's blades against accidental earthquake-type loads using FEM integrated with GA. To the authors' knowledge, PSO-based methodologies have not been applied to the design of jacket structures for OWT.

Taking all of the above into account, this paper proposes a strategy for automating the design of jacket-type support structures for OWTs using a Particle Swarm Optimization (PSO) algorithm with a particular non-random precomputed initial swarm for finding candidate designs that satisfy the considered structural and geometrical requirements with a minimum use of material. Such precomputed initial population is formed, with a very low computational effort, and for different numbers of legs and bays, by concept jacket designs generated based on the procedure proposed by Jalbi and Bhattacharya [24]. Then, the PSO algorithm is coupled to a FE structural model and is used as a search and optimization tool. The proposed strategy takes into account the characteristics of the turbine along with the properties and environmental conditions of the location for which the jacket is designed. The aim of this paper is to generate a set of preliminary candidate designs of the jacket with a level of detail corresponding to the initial phases of design. Compliance with safety standards and guidelines is ensured by checking a wide range of structural requirements, including section capacity, buckling, resonance and joints geometry.

Section 2 describes in detail the proposed strategy. Then, Section 3 defines the problem that will be considered for testing and verification. Section 4 presents the results of the study and analyzes, one by one, aspects such as the influence of the type of initial population, the behavior of the proposed fitness function, the characteristics of the obtained candidate results, or the computational effort involved. Finally, Section 5 summarizes the main conclusions that can be drawn from this study.

2. Methodology

2.1. General overview of the design strategy

The proposed algorithm consists of three main phases: initialization, establishment of an initial population, and optimization process. Fig. 1 presents a flowchart that summarizes the main aspects of the proposed strategy.

During the initialization phase, three types of input data are defined. The first is related to the topology of the jacket and its external dimensions, the second relates to the metocean conditions at the jacket site, and the third to the wind turbine data. The latter two data sets are necessary to define the gravity loads, as well as the loads generated by wind and waves. Section 2.3 provides a detailed explanation of the loads considered.

Then, the PSO is used as a tool for the search and optimization of candidate designs for jacket substructures. PSO is a metaheuristic optimization algorithm that makes use of a population of particles, each of which represents a potential solution. The

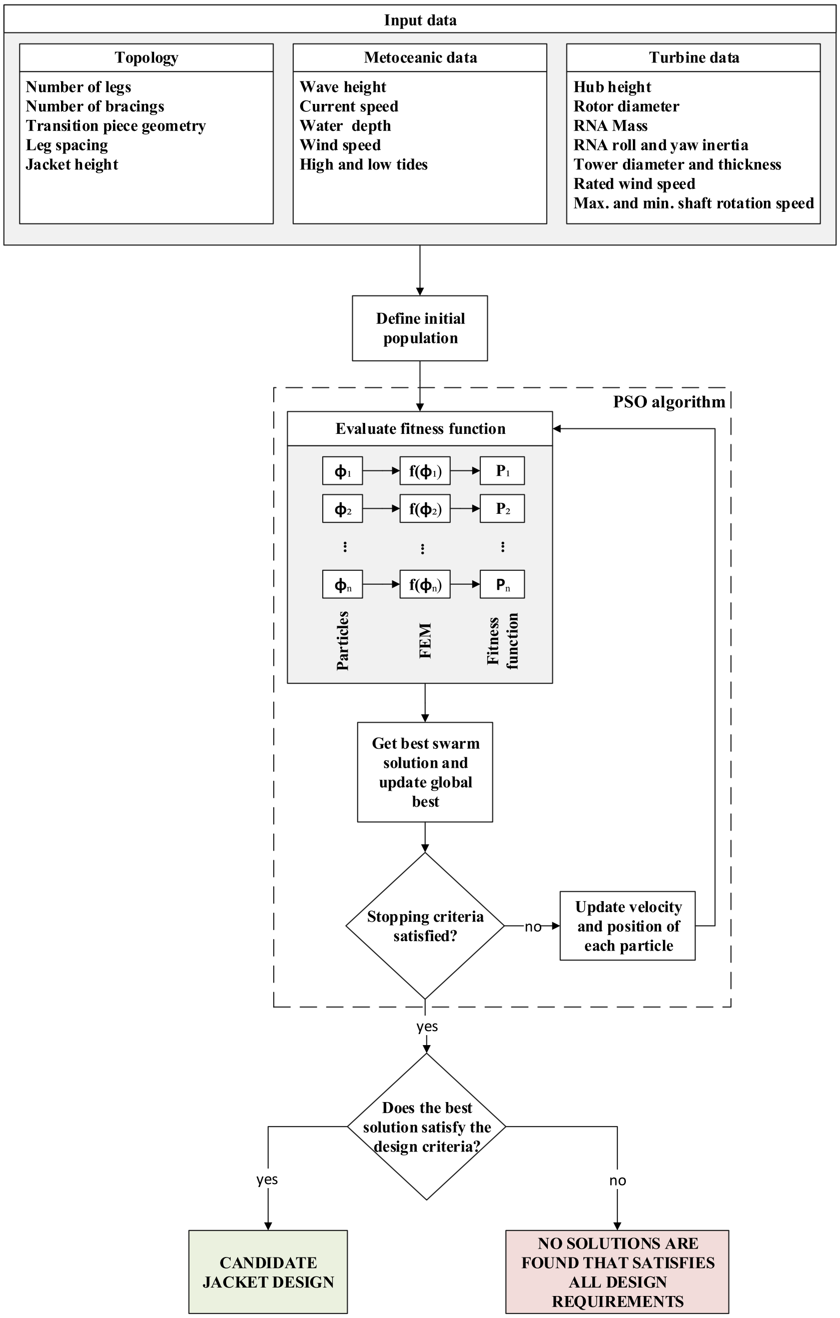

Fig. 1. Overall work-flow of the proposed design strategy.

initial population can be generated randomly or by precomputing preliminary designs that already meet certain requirements. This last option requires a more laborious process but improves the possibility of finding better solutions with less computational effort, as will be shown later. A process for the generation of potential initial solutions that employs the compact expressions provided by Jalbi and Bhattacharya [24] for concept design of OWT jacket foundations is explored in this work. The best particles are selected based on jacket mass and design requirements. Next section presents, in more detail, the different strategies explored for the generation of the initial population. Section 4.1 discusses the significant impact that the quality of the initial population can have on the algorithm's performance.

After having defined the initial population (Section 2.2), the swarm particles are evaluated by the FE model (Section 2.3) to obtain their fitness value. Then, particle velocity and position are updated and the process is repeated until the stopping criterion is satisfied. More details about the PSO algorithm are given in Section 2.4.

2.2. Strategies for determining the initial population

Three different alternatives for the generation of the initial PSO population are explored and evaluated in this paper: (a) the generation of precomputed candidates that already meet design requirements, based on the expressions proposed by Jalbi and Bhattacharya [24]; (b) a completely random initial population; or (c) an initial population consisting of 50% of particles generated through the first approach and 50% of particles randomly generated.

The precomputed population is obtained from the compact expressions for the concept design of jacket-type substructures for OWTs by Jalbi and Bhattacharya [24] which only requires general turbine and environmental data. Although in their work only jackets with 3 or 4 legs were considered, the same approach is assumed for 5-leg systems. The first step is to obtain the bending stiffness of the tower-jacket system ($EI_{\mathrm{T-J}}$) from:

$$EI_{\mathrm{T-J}} = f_{\mathrm{fb}}^2 \cdot \frac{4\pi^2}{3} \cdot (0.243 \cdot m_{\mathrm{eq}} \cdot h_{\mathrm{total}} + M_{\mathrm{RNA}}) \cdot (h_{\mathrm{total}})^3 \tag{1}$$

where f_{fb} is the fixed base natural frequency of the system, m_{eq} the equivalent distributed mass of the jacket-tower obtained from the non-dimensional plot of equivalent mass for a fixed and flexible base described by Jalbi and Bhattacharya [25], h_{total} the combined height of the tower and the jacket, and M_{RNA} the mass of the Rotor Nacelle Assembly (RNA) system. The fixed base natural frequency (f_{fb}) takes values between the rotor frequency (1P) and blade passing frequency (3P) limits. The jacket height (H_{jacket}) is obtained from:

$$H_{\mathrm{jacket}} = H_{\mathrm{w}} + H_{\mathrm{m,50}} + H_{\mathrm{s,50}} \cdot 0.20 \tag{2}$$

where H_{w} is the maximum expected depth of the water, $H_{\mathrm{m,50}}$ the 50-y extreme wave height, and $H_{\mathrm{s,50}}$ the 50-y extreme sea state.

Then, the jacket bending stiffness (EI_{J}) is obtained from:

$$EI_{\mathrm{J}} = \frac{EI_{\mathrm{T}}}{\chi} \tag{3}$$

being:

$$\chi = \frac{1}{\left(1 + \frac{h_{\mathrm{jacket}}}{h_{\mathrm{tower}}}\right)^3 - 1} \cdot \left[\frac{EI_{\mathrm{T}}}{EI_{\mathrm{T-J}}} \cdot \left(\frac{h_{\mathrm{jacket}} + h_{\mathrm{tower}}}{h_{\mathrm{tower}}}\right)^3 - 1\right] \tag{4}$$

where h_{tower} is the tower height, and EI_{T} the tower bending stiffness.

The bending stiffness of the top section of the jacket (I_{top}) can then be found as:

$$I_{\mathrm{top}} = \frac{EI_{\mathrm{J}}}{E \cdot f(m)} \tag{5}$$

where E is the elastic modulus of the jacket material, and $f(m)$ is obtained from:

$$f(m) = \frac{1}{3} \cdot \frac{m \cdot (m-1)^3}{m^2 - 2 \cdot m \cdot \ln(m) - 1} \tag{6}$$

where $m = S_{\mathrm{bottom}}/S_{\mathrm{top}}$, being S_{bottom} the bottom leg spacing, and S_{top} the legs spacing at the top of the jacket. The cross-sectional area of each leg required to maintain the fixed-base fundamental frequency is obtained from the moment of inertia of Eq. (5) as:

$$A_{\mathrm{leg}} = \begin{cases} 2 \cdot (I_{\mathrm{top}}/S_{\mathrm{top}}^2) & \text{if} \quad n_{\mathrm{leg}} = 3 \\ I_{\mathrm{top}}/S_{\mathrm{top}}^2 & \text{if} \quad n_{\mathrm{leg}} = 4 \\ I_{\mathrm{top}}/(S_{\mathrm{top}}^2 \cdot 1,81) & \text{if} \quad n_{\mathrm{leg}} = 5 \end{cases} \tag{7}$$

After computing the required area of the legs, the diameters and thickness are selected within appropriate ranges for each case. In order to ensure optimal joint performance, the diameters and thicknesses of the braces are obtained from ratios compared to those of the legs. Further details can be found in Section 3.4.

2.3. Structural model

At each iteration, the particles are evaluated through a structural FE model implemented by Quevedo-Reina et al. [26]. This model analyses the structural feasibility of the jacket substructure by considering three main aspects: evaluation of external loads (Sections 2.3.1 and 2.3.2), calculation of the structural response (Section 2.3.3), and verification of design requirements (Section 2.3.4).

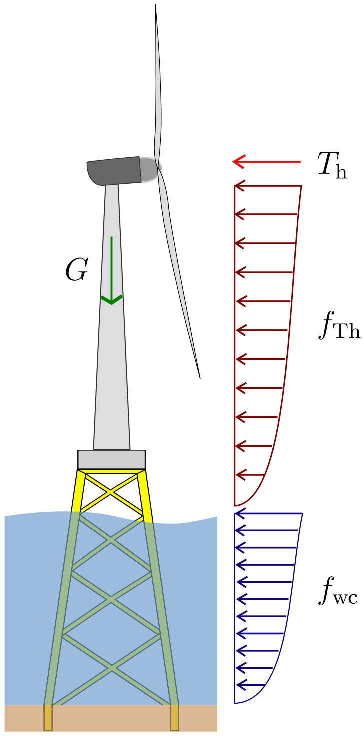

Fig. 2. Representation of gravity, wind, wave, and current loads acting on the OWT-jacket system.

2.3.1. Design loads

The design loads considered by the structural model are divided in two main groups; (1) the gravitational loads associated to the weight of all structural elements and the buoyancy of submerged elements and (2) the environmental loads acting on the structure produced by the drag forces of wind, currents, and waves. A visual representation of the loads acting on the system is shown in Fig. 2, where G represents the gravity load, T_h the wind load acting on rotor, f_Th the wind load acting on the tubular members, and f_wc the wave and currents loads acting on the jacket tubular members. Accidental loads such as those produced by earthquakes or ice impact are not taken into account.

Wind load evaluation

Wind loads are considered to be quasi-static and are composed of the average wind speed and the turbulent component. The thrust force acting on the RNA is estimated following Arany et al. [27] as:

$$T_\mathrm{h} = \frac{1}{2}\rho_\mathrm{a} A_R C_T U^2 \tag{8}$$

where ρ_a is the air density, A_R the rotor area, C_T the thrust coefficient, proposed by Frohboese et al. [28] for estimating wake effects in fatigue loading calculations. The wind speed U is the sum of the average wind speed ($\bar{U}$) and the turbulent component (u) as: $U = \bar{U} + u$. This formulation aims to simplify the complex thrust forces received by the blades, analyzing the RNA as a whole. For the remaining elements, including the tower and jacket top, a distributed load is applied along the members, following the international standard DNVGL-RP-C205 [29]:

$$f_\mathrm{Th} = \frac{1}{2}\rho_\mathrm{a} D_i \sin(\alpha) C_D U(z)^2 \tag{9}$$

being C_D the drag coefficient, D_i the diameter of member i, α the angle formed between the wind direction and the normal direction to the exposed surface, and $U(z)$ the wind speed at the specific height.

Wave and current load evaluation

Wave forces are calculated using Morison's equations [30]. The loads generated by both waves and currents can be segregated into three categories: loads produced by waves, loads produced by currents due to wind, and loads from the action of circulating currents. These three loads are summed up over the entire height of the submerged section of the jacket, as defined by Arany et al. [27]:

$$f_\mathrm{wc} = \frac{1}{2}\rho_\mathrm{w} C_D |v_n| v_n + \frac{1}{4}\rho_\mathrm{w}\pi D_i^2 C_M \dot{v}_n \tag{10}$$

Table 1
Load cases considered by the structural model.

Scenario	Wind model	Wave model	Alignment
E1	Normal Turbulence Model at nominal wind speed	1-y Extreme Sea State	Collinear
E2	Extreme Turbulence Model at nominal wind speed	50-y Extreme Wave Height	Collinear
E3	Extreme Operating Gust at nominal wind speed	1-y Extreme Wave Height	Collinear
E4	Extreme Operating Gust at cut-off wind speed	50-y Extreme Wave Height	Collinear
E5	Extreme Turbulence Model at nominal wind speed	50-y Extreme Wave Height	Misaligned 90°

where ρ_{w} is the water density, C_M the inertia coefficient, υ_n and $\dot{\upsilon}_n$ the normal component of the velocity and acceleration respectively of the water particle.

2.3.2. Load cases

Numerous load cases are proposed by the international standard DNV GL-ST-0437 [31] for the design of supporting structures for OWT. The aim is to ensure that the lifetime of the system is, at least, 30 years. The structural model considers the five most representative scenarios for the design according to Arany et al. [27], which are summarized in Table 1.

2.3.3. Finite element model

The structural response is obtained through a previously developed FE model [26], which performs an equivalent static analysis of the jacket response under the influence of external loads, specified in Section 2.3.1. Each element of the substructure (braces and legs) is modeled using Timoshenko's beam theory [32], with rigid connections assumed at the joints. The platform is assumed to be a rigid element which links the upper sections of the legs. Additionally, the jacket legs are considered fixed to the seabed. Therefore, once the discretization is built, and the external forces ($\boldsymbol{f}_{\mathrm{ext}}$) are computed as stated in Section 2.3.1, a system of equation of the type: $\boldsymbol{K} \cdot \boldsymbol{u} = \boldsymbol{f}_{\mathrm{ext}}$ is solved, with $\boldsymbol{K}$ being the global stiffness matrix and $\boldsymbol{u}$ the vector of nodal displacements.

Wind loads are considered as quasistatic loads, covering their variability by the different load cases. However, waves loads can induce relevant dynamic effects. In that case, following the recommendation of Arany et al. [27] a Dynamic Amplification Factor (DAF) is used for incrementing waves loads:

$$\mathrm{DAF} = \frac{1}{\sqrt{\left(1-\left(\frac{1}{T_{\mathrm{wave}} f_{\mathrm{n}}}\right)^2\right)^2 + \left(\frac{2\xi_{\mathrm{n}}}{T_{\mathrm{wave}} f_{\mathrm{n}}}\right)^2}} \tag{11}$$

where T_{wave} is the wave period, f_{n} the system natural frequency, and ξ_{n} the modal damping coefficient.

The dynamic characterization of the system is conducted by solving the eigenvalue problem as:

$$|\bar{\boldsymbol{K}} - \bar{\omega}^2 \boldsymbol{M}| = \boldsymbol{0} \tag{12}$$

where $\bar{\omega}$ denotes a complex natural frequency of the system, $\bar{\boldsymbol{K}}$ is the complex stiffness matrix, and $\boldsymbol{M}$ is the mass matrix. Hysteretic material damping is assumed for the structural elements through complex valued material properties of the type: $\bar{E} = E(1 + 2\mathrm{i}\xi_n)$. In case of submerged elements, material damping coefficient is incremented in 1% to introduce the energy dissipation owing to water–structure interaction. The aeroelastic damping generated between the wind and the rotating blades is considered through punctual hysteretic dampers at rotor level for the fore-aft and side-to-side directions. The mass matrix is built by considering the inertial behavior of the structural elements. Additionally, the water-structure interaction of the submerged elements is modeled as a distributed added mass that represents the effect of the water mass inside the tubular section and of the interaction with the surrounding water (according to DNVGL-RP-C205 [29]) as:

$$m_{\mathrm{w}} = \frac{\pi \rho_{\mathrm{w}}}{4} \cdot \left[\left(D_i - 2t_i\right)^2 + C_A D_i^2\right] \tag{13}$$

where $C_A = 1$ is the added mass coefficient.

2.3.4. Structural verifications

This section describes the different structural verifications considered in this study, performed as defined in Quevedo-Reina et al. [26]. Table 2 contains a summary of the considered verifications and criteria. The section capacity of all structural elements are evaluated using the von Mises stress criterion. The column and shell buckling resistance is checked in accordance with the international standard DNVGL-RP-C202 [33]. For column buckling, an effective length factor of 1 (pinned-pinned beam) is assumed. In accordance with the international standard DNVGL-ST-0126 [34] to prevent fatigue damage, the natural frequencies of the system are placed away from the rotor and blade-passing frequencies. Finally two geometric restrictions are established: a minimum jacket height according to DNVGL-ST-0126 [34] and constraints in welded unions extracted from Appendix B of DNVGL-RP-C203 [35] to avoid unrealistic joints.

All these verifications are represented by partial utilization factors (γ_j) that allow a direct comparison between them. A unitary value of the utilization factors indicates maximum utilization, while larger values indicate that the requirement is not fulfilled. A global utilization factor is then defined as the maximum of all of the obtained partial utilization factors ($\gamma = \max(\gamma_j)$).

Table 2
Verifications implemented in the structural model.

Verification	Description	Criterion
Ultimate Limit States (ULS)	Section capacity	von Mises
	Column buckling	DNVGL-RP-C202 [33]
	Shell buckling	DNVGL-RP-C202 [33]
Fatigue Limit State (FLS)	Frequency study	DNVGL-ST-0126 [34]
Geometric restrictions	Platform height	DNVGL-ST-0126 [34]
	Welded unions	DNVGL-ST-C203 [35]

2.4. Particle swarm optimization algorithm

PSO is a global stochastic optimization algorithm inspired by the social behavior of schools of fish and flocks of birds. The algorithm was develop by Kennedy and Eberhart in 1995 [36,37]. The PSO algorithm enables exploring vast candidate solution spaces without making assumptions about the optimized issue. Nevertheless, the algorithm cannot guarantee finding the optimal solution. PSO aims to find a valid solution that maximizes or minimizes a specified objective function.

Each particle is defined by the vector $\vec{\phi}$ containing the variables to be optimized. Upper $\left(\overline{\phi_i}\right)$ and lower $\left(\underline{\phi_i}\right)$ boundary values are established for these variables. In general terms, the optimization process carried out by the PSO-based automatic design algorithm is defined as follows:

$$\begin{aligned} \text{find:} \quad & \vec{\phi} = \left[\phi_1, \ldots, \phi_{n_{\text{var}}}\right] \\ \text{to minimize:} \quad & f(\vec{\phi}) = \rho_{\text{m}} \sum_{e=1}^{n_e} A_e \cdot l_e \\ \text{subject to:} \quad & \underline{\phi_i} \le \phi_i \le \overline{\phi_i} \qquad i = [1, \ldots, n_{\text{var}}] \\ & \gamma_j \le 1 \qquad j = [1, \ldots, n_{\text{req}}] \end{aligned}$$

where ρ_{m} is the steel density, A_e and l_e the cross-sectional area and length of the e element, and γ_j the utilization factor corresponding to the jth requirement of a total of n_{req}.

To minimize the objective function $f(\vec{\phi})$, a fitness function is required to assign each particle a fitness value. In this work, the fitness function is a two-stages conditional function that guides the design process towards feasible designs and to jacket mass optimization. First of all, the particle undergoes evaluation in the FEM, and the jacket mass and global utilization factor are computed. If the population does not contain the minimum percentage of candidates that meet all the requirements, r_γ, the fitness function is based exclusively on the global utilization factor to guide the optimization in the search for feasible designs. Once this minimum percentage is reached, the fitness function moves on to optimizing the jacket mass. Function 1 defines the fitness function used in this work,

Function 1 Fitness Function.

procedure FEM evaluation
  return m_{jacket} and γ
end procedure
if $c_\gamma < r_\gamma \cdot n_{\text{particles}}$ **then**
  FFO $= \gamma \cdot \iota$
else
  if $\gamma \le 1.00$ **then**
    FFO $= m_{\text{jacket}}$
  else if $\gamma > 1.00$ and $\gamma \le \kappa$ **then**
    FFO $= \gamma \cdot (m_{\text{jacket}} + \delta)$
  else if $\gamma > \kappa$ **then**
    FFO $= \gamma \cdot (m_{\text{jacket}} + \delta) \cdot e^{(\gamma-\kappa)}$
  end if
end if

where FFO is Fitness Function Output, c_γ represents a counter that record the number of particles in the population that meet the design requirements, m_{jacket} the jacket mass, r_γ the ratio of swarm particles that must meet all design requirements before proceeding to mass optimization, and ι, κ and δ are parameters used to penalize individuals who do not meet the design requirements but, at the same time, give them the possibility to evolve towards compliance.

The control of the motion of the particle in the PSO can be decomposed into position ($\vec{\phi}$) and velocity ($\vec{v}$) vectors. Essentially, a particle's position represents a potential solution to the optimization problem, while its velocity indicates the direction and magnitude of its movement within the search space. Each particle relocates itself to a different position at each iteration (τ). The position in each iteration, other than the first one ($\tau \neq 0$) is determined as follows:

$$\vec{\phi}_i^{\tau+1} = \vec{\phi}_i^{\tau} + \vec{v}_i^{\tau+1} \tag{14}$$

Table 3
Properties of the NREL 5-MW OWT [14].

Parameter	Value
Rating [MW]	5.0
Rotor orientation	Upwind
Configuration	3 blades
Rotor diameter (D_{rotor}) [m]	126.0
Hub height from top of transition piece (H_{hub}) [m]	70.0
Cut-in (V_{in}), cut-out (V_{out}), rated wind speed (V_n) [m/s]	3.0, 25.0, 11.4
Cut-in (f_{min}), rated rotor speed (f_{max}) [rpm]	6.9, 12.1
RNA mass (M_{RNA}) [kg]	$3.50 \cdot 10^5$
Inertia RNA roll ($I_{RNA,roll}$) [kg m^2]	$3.54 \cdot 10^7$
Inertia RNA yaw ($I_{RNA,yaw}$) [kg m^2]	$2.30 \cdot 10^7$
Top tower diameter (D_{top}) [m]	4.0
Bottom tower diameter (D_{bottom}) [m]	5.6
Top tower thickness (T_{top}) [mm]	30.0
Bottom tower thickness (T_{bottom}) [mm]	32.0
Tower height (H_{tower}) [m]	68.0

where $\vec{v}_i^{\,\tau+1}$ represents the velocity of the particle of the ith particle for computing its new position, and is determined as:

$$\vec{v}_i^{\,\tau+1} = \xi \cdot \vec{v}_i^{\,\tau} + u_{1,i}^{\tau} \cdot r_1 \cdot \left(\vec{\phi}_{i,\text{local best}}^{\,\tau} - \vec{\phi}_i^{\,\tau}\right) + u_{2,i}^{\tau} \cdot r_2 \cdot \left(\vec{\phi}_{i,\text{global best}}^{\,\tau} - \vec{\phi}_i^{\,\tau}\right) \tag{15}$$

where ξ is the inertia or control parameter, $u_{1,i}^{\tau}$ and $u_{2,i}^{\tau}$ are independent random numbers, and r_1 and r_2 are the acceleration coefficients used to guide the particle to its best local position or to the best global position of the swarm, respectively. Three addends are distinguished in Eq. (15). The first term is the inertial component and regulates the particle's trajectory smoothly, avoiding abrupt changes. Low values of ξ ($\xi \ll 1$) favor exploration by giving more weight to the individual knowledge of each particle. Bringing $\xi \approx 1$ cause the particles to slow down in the search space and the new velocity to be in sync with the previous iteration's velocity. Very high values ($\xi \gg 1$) can lead to divergences and areas of the search space not being explored. The second term symbolizes the cognitive component of the particle. It is also known as the self-adjusting weight part, as it refers to the local best position the particle has found. High values of r_1 causes the particle to be guided to the best position it has found. Finally, the third term represents the social component. It considers the optimal position of nearby particles. High values of r_2 means that the particle tends to go to the global best position that the swarm has found. For the initial iteration ($\tau = 0$), the velocities are randomly generated within established boundaries ($\pm v_{\max}^{\tau=0}$), and the particle positions correspond to the initial population ($\vec{\phi}_i^{\,\tau=0}$).

In order to complete the process, the algorithm requires a stopping criterion that yield the ultimate solution. The criteria that can be taken into account include: reaching a maximum number of iterations, exceeding a maximum computational time, reaching a predefined objective value for the best solution, or not improving the best solution for a predefined number of iterations.

The methodology presented in this article is developed in the MATLAB programming language [38]. Specifically, the PSO algorithm is implemented in the optimization package as a modification suggested by Mezura-Montes and Pedersen [39,40].

3. Problem definition

3.1. Reference OWT

The wind turbine used to validate the proposed methodology is the well-established NREL-5MW wind turbine, as described by Jonkman et al. [14]. It is a 3-blade wind turbine with a rated power of 5 MW. Hub Height (H_{hub}) is 70 m high, 90.55 m above mean sea level, and the tower (H_{tower}) is a 68 m high conical steel structure. All turbine parameters are listed in Table 3 and some of the variables are shown in Fig. 3, where β_{br} is the angle formed by the braces. The aeroelastic damping ratios are assumed to be 6% for the fore-aft direction and 0.75% for the side-side direction.

3.2. Reference jacket for comparison and validation

The support structure used as a reference for the validation of this methodology is defined as proposed by the IEA Wind Task 30 "Offshore Code Comparison Collaboration Continuation" (OC4) Project - Phase I [13]. This OC4 reference jacket was designed for the conditions in the Dutch North Sea by Vemula et al. [41], but was adapted and simplified for the OC4 project. A three-dimensional representation of the OC4 jacket is shown in Fig. 4. The geometric values of the jacket bars are given in Table 5. The color coding in the figure and in the table helps to identify the geometric dimensions of each element.

This OC4 jacket is a lattice structure with four legs, divided in height by four braces, also known as bays or levels, with X-Type geometry. The legs of the OC4 jacket have the same diameter throughout their length, but the thickness varies at each brace interval. The bracings of the OC4 has the same diameter and thickness along its length and in each bay section. The height of the jacket (H_{jacket}) is 66.15 m, with an upper leg spacing (S_{top}) of 8 m, and a lower leg spacing (S_{bottom}) of 12 m. The transition piece is a reinforced concrete block that covers the entire top surface of the jacket. It has a 4-m edge (H_{TP}) and weight 666 tons. The jacket's weight (m_{jacket}), excluding the transition piece, is 535 tons. All material properties are listed in Table 4.

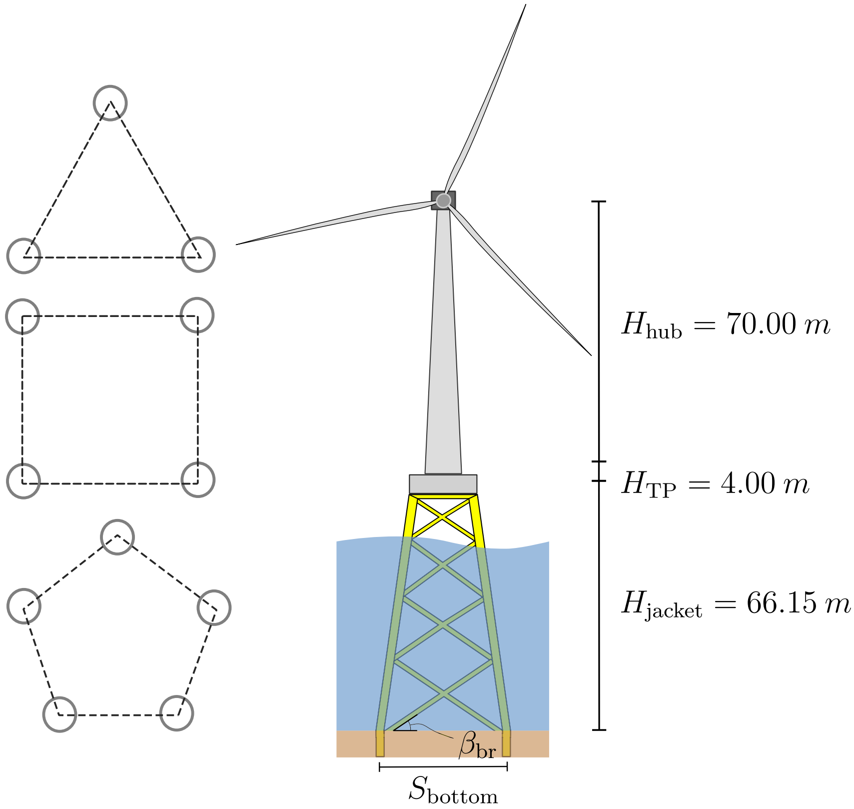

Fig. 3. Representation of a jacket supported OWT, the nomenclature used and the three possible leg configurations.

Table 4
Material properties.

Parameter	Value
Young's modulus (E) [GPa]	200
Poisson's ratio (ν)	0.30
Density (ρ) [kg/m^3]	7850
Yield stress (f_{yield}) [MPa]	355
Material damping (ξ_n)	0.5%

Table 5
Geometric dimensions of the OC4 jacket.

Component	Color in Fig. 4	Diameter [m]	Thickness [mm]
Bracings	Purple	0.80	20
Legs section 1	Yellow	1.20	40
Legs section 2	Blue	1.20	35
Legs section 3	Red	1.20	50
Pile	Green	2.08	60

3.3. Site conditions

Table 6 presents all the values assumed in this study for the metocean conditions at the location of the OWT site.

3.4. Design variables, constraints and PSO settings

The variables subject to change by the PSO during the design process are those related to the geometry of the jacket, gathered in vector $\vec{\phi}$ as follows:

$$\vec{\phi} = \left(D_{\text{leg},1},\, t_{\text{leg},1},\, D_{\text{br},1},\, t_{\text{br},1},\, \ldots,\, D_{\text{leg},\text{n}_{\text{br}}},\, t_{\text{leg},\text{n}_{\text{br}}},\, D_{\text{br},\text{n}_{\text{br}}},\, t_{\text{br},\text{n}_{\text{br}}},\, S_{\text{bottom}} \right) \in \mathbb{R}^{n_{\text{var}}} \tag{16}$$

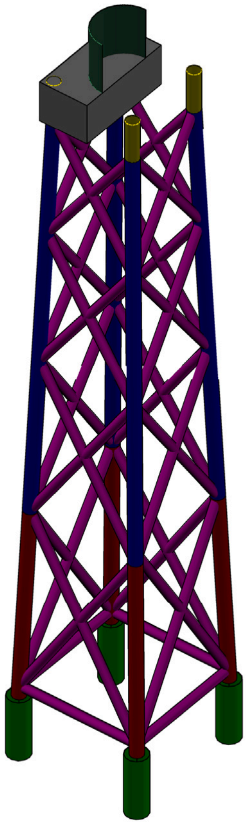

Fig. 4. Three-dimensional representation of the OC4 jacket [13] with a color code to determine the dimensions of the elements listed in the Table 5.

Table 6
Environmental conditions for load calculation.

Parameter	Value	Description
$H_{s,1}$ [m]	7.10	1-y Extreme Sea State
$H_{s,50}$ [m]	9.40	50-y Extreme Sea State
$H_{m,1}$ [m]	13.21	1-y Extreme Wave Height
$H_{m,50}$ [m]	17.48	50-y Extreme Wave Height
$V_{current}$ [m/s]	0.60	Historical average sea current velocity
V_{wind} [m/s]	6.47	Average wind speed at 10 m mean sea level
$k_{Weibull}$	2.04	Weibull distribution shape parameter

where D and t represents the outer diameter and thickness of the bars (legs and braces) and S_{bottom} the bottom leg spacing. These design-dependent variables and their upper and lower limits are listed in Table 7. This data vector with the design variables is evaluated in the fitness function (see Function 1) assuming the following values for its parameters: $r_\gamma = 0.1$, $\iota = 10^{10}$, $\kappa = 1.50$, and $\delta = 10^7$. The rest of structural and non-structural elements of the system (RNA, tower and transition piece, including the parameters S_{top} and H_{TP}) are kept as defined in Sections 3.1 and 3.2.

Jackets with 3 to 5 legs, and 3 to 5 bays are considered. X-type braces are always assumed. Jackets featuring X-type braces provide greater structural rigidity in comparison to the Pratt type (single diagonal) [42]. In addition, Puyang et al. [43] has carried out a study ensuring that the X-type braces perform better under dynamic loads compared to the Z or K types. The jacket top geometries that are adopted depending on the number of legs for the jackets are: symmetrical triangles for 3 legs, squares for 4 legs, and pentagons for 5 legs (see Fig. 3). Two design alternatives are studied: the first assumes that the diameter of the legs is constant along their length, but the thickness varies in each bay section; and the second allows the algorithm to vary both the thickness and diameter at each level. The diameter and thickness of the bracings remain constant along their length in the bay. The crown surrounding all the legs at the last level of the jacket near the connection with the piles (see Fig. 4) is not taken into account as the joint is assumed rigid.

A total of 18 different jacket topologies are considered. These topologies results from the combination of the number of legs (3, 4 or 5), number of braces (3, 4 or 5) and leg diameter variation (constant along their length or different for each bay level). Due

Table 7
Lower and upper limits of the design-dependent variables used in the algorithm design process.

Variable	Lower limit [m]	Upper limit [m]
$S_{\text{bottom 3-legs}}$	12.6	38
$S_{\text{bottom 4-legs}}$	8.0	24
$S_{\text{bottom 5-legs}}$	5.8	18
D_{leg}	0.50	4.60
D_{br}	0.15	2.50
t_{leg}	0.008	0.15
t_{br}	0.005	0.08

to the metaheuristic nature of the PSO, each topology is run a total of 4 times, i.e., the total number of runs is 72. The population size is set to 40 and the maximum number of iterations without observed improvement in the FFO has been set to 30.

The precomputed initial populations are generated according to what is described in Section 2.2 and considering, for the present case, $0.29 \leq f_{\text{fb}} \leq 0.31$ Hz, $1.5 \leq D_{\text{leg}_i} \leq 3.0$ m, and $2° \leq \alpha_{\text{leg}} \leq 8°$. The thicknesses of the legs (t_{leg_i}) are deduced from the cross-section area, that is obtained from Eq. (7), and from the proposed leg diameter range (D_{leg_i}). The diameters of the braces (D_{br_i}) are obtained from the ratio $D_{\text{br}}/D_{\text{leg}} = 0.4$ recommended by Chakrabarti [44] to achieve satisfactory adhesion and optimal performance of the connections. Finally, a range of values for the thickness of the braces (t_{br_i}) is obtained by assuming a ratio $D_{\text{br}}/t_{\text{br}}$ between 40 and 60 as recommended by McClelland and Reifel [45]. By generating all possible variables and ranges, approximately 9000 candidates are produced for each combination of leg and brace numbers (note that for both the constant and bay-variable leg diameter cases the same initial population is used). The entire set is evaluated and the best 40 candidates in terms of jacket mass (prioritizing those that comply with the structural requirements) are selected.

4. Results

4.1. Influence of the initial swarm

To determine the best initial population approach, a study is first conducted for the specific topology of the reference OC4 jacket, which consists of 4 legs and 4 braces. The three alternative strategies described in Section 2.2 for the generation of the initial population are explored. This is done for the two alternatives for the leg designs (constant diameter from top to bottom, or piecewise diameter by bays). Four runs are executed for each of the resulting possibilities, which makes up a total of 24 independent runs for this test. A unique set of precomputed particles is used in all runs with a precomputed initial population. In order to illustrate the difference between the random, in blue, and the precomputed, in green, approaches, Fig. 5 presents the comparison between the global utilization factor of the 40 particles of two initial populations corresponding to both approaches at the first iteration. It can be seen that the random approach has greater values for the global utilization factor than the precomputed one. In addition, the random candidates gives the algorithm greater heterogeneity, with a wide range of different utilization factors. This is beneficial from the algorithm's point of view, as the particles have more information about the search space.

The optimization strategy switch is one of the most important factors in the behavior of this algorithm, as it may become stuck in the first strategy while searching for feasible candidate structures that satisfy all structural requirements. In order to illustrate the evolution of the best solutions, Fig. 6 displays the Fitness Function Output (FFO) value for the best candidate solution of the population at each iteration. The figure represents all runs with the 24 case studies for the 3 initial population proposed: precomputed in green, random in blue, and mixed in brown. The dashed lines represent the variable leg diameter jackets at each bay section, and the solid one the constant leg diameter study. Additionally, the mass of the reference OC4 jacket is provided to serve as a comparison with the obtained solutions.

Candidates solutions lighter than the OC4 reference jacket are found for the proposed loading conditions and structural checks in 4 out of the 8 cases analyzed, all from precomputed initial population. The change from searching enough feasible designs to optimizing for minimum total mass is clearly observed in Fig. 6 by the fall in the FFO from around 10^{10} to 10^{5}. It is also observed that, in three of the runs, not enough feasible candidate solutions were found before reaching the stopping criterion, despite belonging to the initial precomputed population studies. It is also observed that runs with precomputed initial populations tend to need a higher number of iterations to reach the necessary proportion of feasible structural candidates but, in turn, once they do so, they consistently reach significantly better solutions in terms of structural mass.

Based on the analysis, the precomputed initial population option emerges as the best strategy for building the initial populations. For this reason, this is the strategy that will be used when obtaining all the results presented in the next sections.

4.2. Mass results and geometric values

This section summarizes the final results obtained using the methodology described in the previous sections for the problem at hand.

First, Fig. 7 presents the results in terms of total mass of the candidate jacket designs, for the 18 studied configurations combining number of legs, number of braces, and type of leg. For each one of these combinations, the best candidate solution reached for each one of the 4 runs is presented as one individual bar. The red bars indicate that the solution obtained did not meet the design

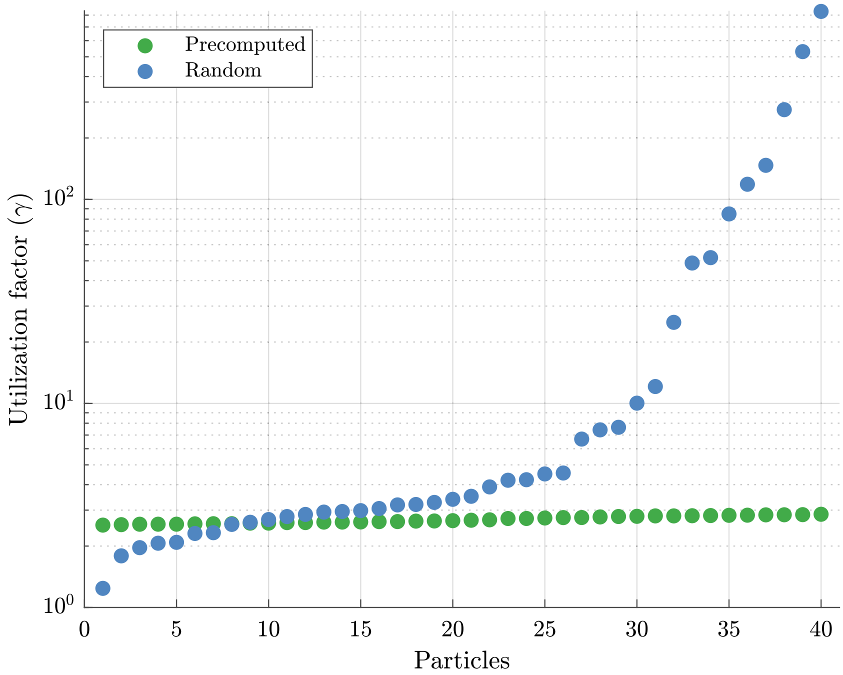

Fig. 5. Global utilization factor (γ) of the first iteration for the 40 random and 40 precomputed candidates.

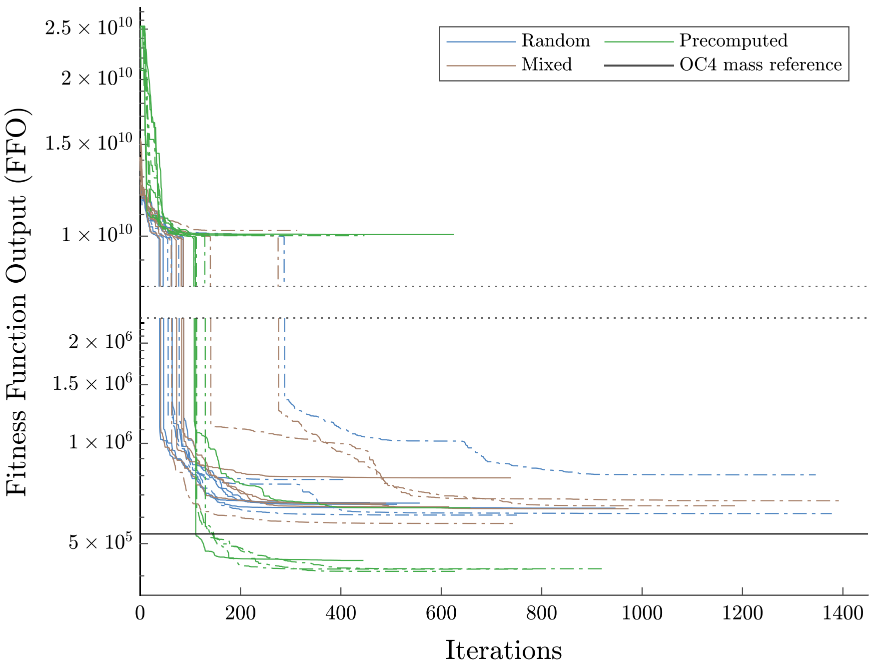

Fig. 6. Evolution of the FFO at each iteration, for the 24 runs with the random, precomputed and mixed initial candidates, and for constant (solid line) and variable (dashed line) leg diameter.

requirements, while the gray bars indicate that the requirements were met. The mass of each jacket is represented by the height of the corresponding bar, with the mass of the best candidate solution that meets the design requirements of each geometric combination shown above each bar. The automatic design algorithm successfully find 34 candidate solutions that met the design criteria for 5 geometric configurations for the constant leg and 6 geometric configurations for the variable leg diameter. However, it was not able to find solutions that met the design criteria for 3 braces neither for constant or variable leg diameter. The global utilization factor

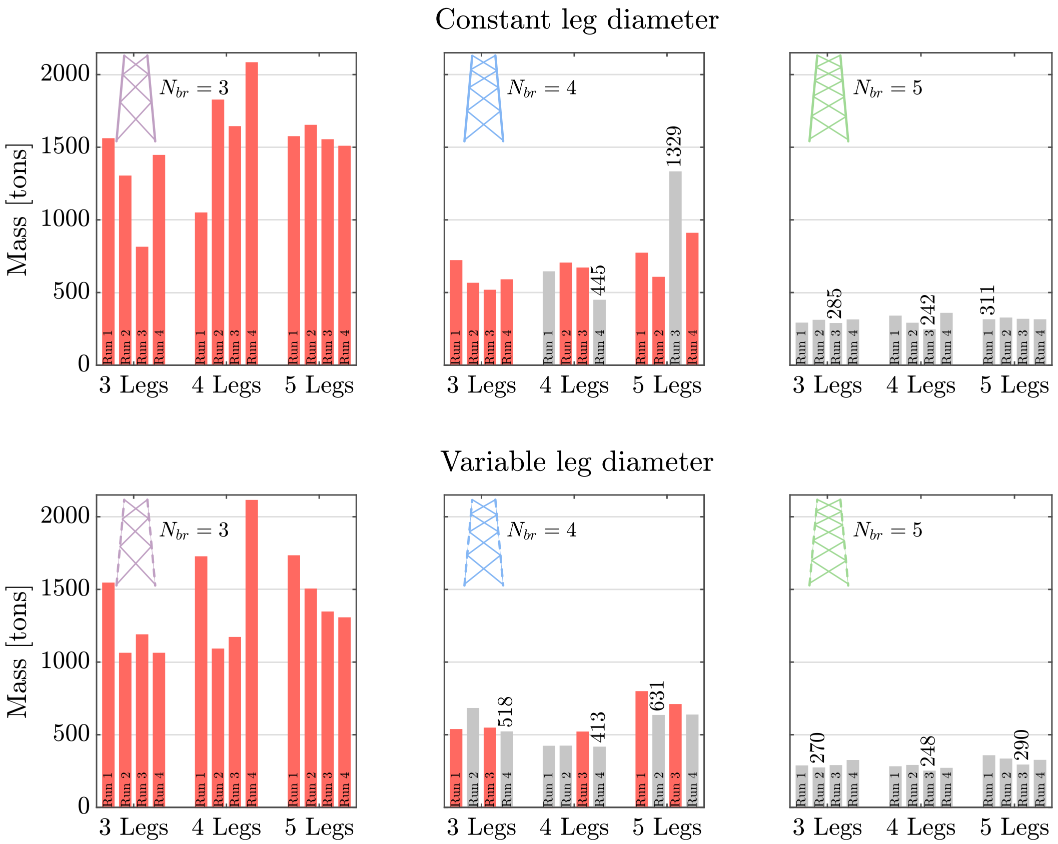

Fig. 7. Relationship between geometric ratios and jacket mass. Red bars represent candidate solutions that do not meet the design requirements, while gray bars represent feasible solutions. The values above the bars correspond to the mass of the best candidate for each geometric configuration. One bar is presented for each individual run of the whole methodology for each topology.

for the solutions presented in Fig. 7 that meet the design requirements are within a very narrow range close to 1: $0.99 \leq \gamma \leq 1.00$. For non-compliant jackets, the range is $1.01 \leq \gamma \leq 1.15$.

The number of braces has a significant influence on the structural behavior of the system and on the final mass of the jacket. A higher number of braces does not necessarily lead to heavier jackets. For the validation of this methodology and for the given environmental conditions and checks, jackets with 5 braces are more competitive in terms of mass than those with 3 or 4 braces. The proposed procedure has been able to find more solutions that met the design requirements for a greater number of geometric configurations in the variable leg diameter assumption compared to the constant leg diameter assumption. This can be explained as the variable leg diameter designs present a larger number of design variables and, therefore, allow more possibilities to be explored during the optimization process.

Fig. 8 shows the candidates ordered by mass, from lightest to heaviest, that meet the design requirements. A dashed line indicates the mass of the OC4 reference jacket for comparison. Jackets with 3 legs are represented as triangles, those with 4 legs as squares, and those with 5 legs as circles. Those with 4 braces are shown in blue, and those with 5 braces are shown in green. To distinguish between the constant and variable leg diameter study in each bay section, filled symbols (constant leg diameter) and empty symbols (variable leg diameter) are used. Jackets with 3 braces are not shown as no solutions met the design requirements for these topologies. The candidate with 4 legs and 5 braces with constant leg diameter is discarded due to its excessive weight compared to the other options. Solutions obtained with 5 braces are lighter than the 4 braces ones, for the environmental conditions and checks discussed in Section 2. Additionally, all geometric configurations involving 5 bracings (regardless the number of legs) meet the design requirements, unlike those with 3 and 4 braces. In the specific geometric case of the OC4 with 4 legs and 4 braces, and considering its mass to be around 535 tons, the proposed procedure has been able to find alternative solutions that, for the checks imposed, improve the OC4 mass. The algorithm has been able to find solutions in one out of four possible scenarios for the constant leg diameter, and in three out of four possible scenarios for the variable leg diameter. Although solutions with geometric configurations other than the reference OC4 jacket cannot be directly compared, the proposed algorithm has generated candidates with alternative topologies that improve it in terms of mass. It has been observed that incorporating a greater number of braces contributes to reducing the structure's mass by achieving a more efficient distribution of internal forces and decreasing buckling lengths. In contrast, increasing the number of legs does not have a significant impact on the system's mass.

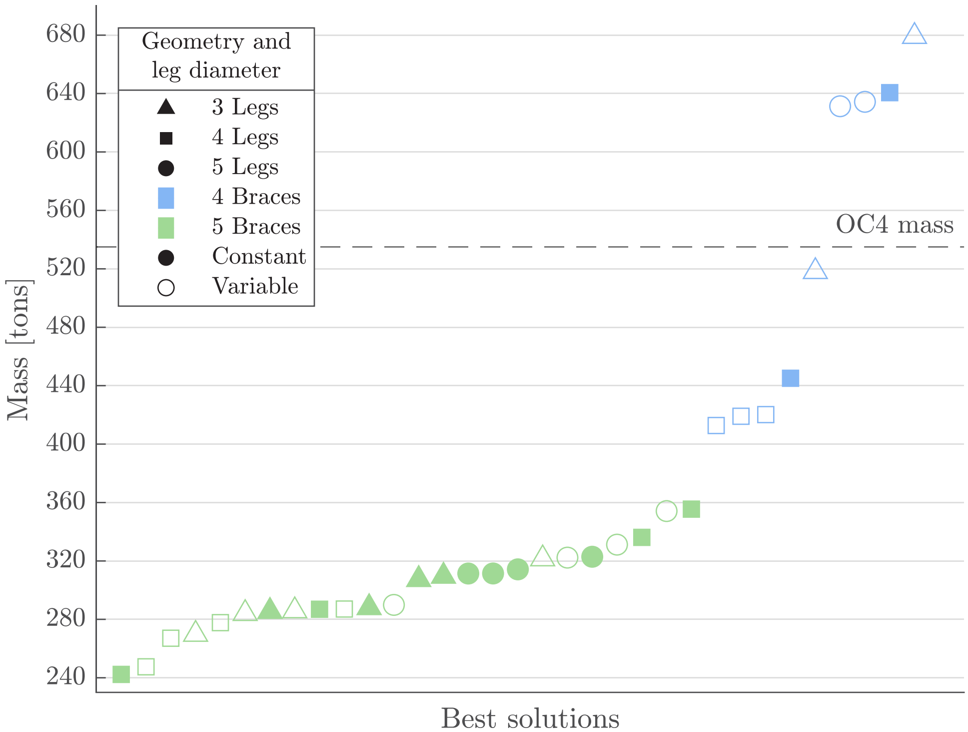

Fig. 8. Jacket mass and geometric configurations for the 33 cases analyzed.

Table 8
Values of the design variables of the lightest candidates by topology.

	C1	C2	C3	C4	C5	C6	C7	C8	C9	C10	C11
n_{leg}	3	4	4	5	5	3	3	4	4	5	5
n_{br}	5	4	5	4	5	4	5	4	5	4	5
S_{bottom} [m]	28,7	16,5	19,9	6,5	15,3	13,3	30,3	17,4	19,4	12,5	14,3
$D_{leg,1}$ [m]	1,15	1,31	0,99	1,34	0,85	1,31	1,19	1,58	0,97	1,80	1,38
$t_{leg,1}$ [mm]	23,8	41,6	33,9	83,7	46,4	81,5	22,9	30,4	33,9	31,3	22,6
$D_{br,1}$ [m]	0,63	0,90	0,52	1,34	0,49	0,87	0,76	0,57	0,57	1,33	0,46
$t_{br,1}$ [mm]	13,9	15,6	12,3	70,3	13,1	21,5	13,2	22,6	9,1	20,7	17,7
$D_{leg,2}$ [m]	1,15	1,31	0,99	1,34	0,85	1,22	1,01	1,34	0,70	1,38	1,17
$t_{leg,2}$ [mm]	17,9	26,2	24,0	66,7	31,5	45,3	23,3	21,8	43,8	27,0	18,6
$D_{br,2}$ [m]	0,48	0,59	0,52	0,87	0,38	0,54	0,64	0,69	0,47	0,62	0,58
$t_{br,2}$ [mm]	16,5	15,0	9,3	36,7	18,1	22,0	11,1	11,9	9,1	26,9	10,7
$D_{leg,3}$ [m]	1,15	1,31	0,99	1,34	0,85	1,24	1,15	1,25	0,88	1,19	0,97
$t_{leg,3}$ [mm]	18,0	23,9	18,5	37,8	24,9	38,9	20,8	22,9	23,9	22,0	18,7
$D_{br,3}$ [m]	0,52	0,46	0,51	0,75	0,37	0,83	0,50	0,50	0,34	0,56	0,39
$t_{br,3}$ [mm]	11,4	22,7	8,4	22,0	12,4	15,0	10,9	21,8	13,6	16,1	12,8
$D_{leg,4}$ [m]	1,15	1,31	0,99	1,34	0,85	1,17	1,11	1,13	0,85	1,09	0,82
$t_{leg,4}$ [mm]	23,5	23,6	18,3	39,3	19,7	61,3	15,3	24,1	20,2	23,6	19,9
$D_{br,4}$ [m]	0,42	0,79	0,33	0,92	0,31	0,89	0,73	0,93	0,44	0,85	0,29
$t_{br,4}$ [mm]	14,2	21,6	9,7	33,5	9,1	22,2	11,4	18,6	10,0	14,4	10,8
$D_{leg,5}$ [m]	1,15	–	0,99	–	0,85	–	1,18	–	0,72	–	0,80
$t_{leg,5}$ [mm]	23,5	–	19,1	–	22,6	–	19,6	–	26,6	–	23,6
$D_{br,5}$ [m]	1,05	–	0,50	–	0,38	–	0,77	–	0,57	–	0,38
$t_{br,5}$ [mm]	23,5	–	10,9	–	8,7	–	19,6	–	10,2	–	9,2
m_{jacket} [tons]	285	445	242	1329	311	518	270	413	248	631	290

Table 8 presents the values of design variables of the lightest candidates for constant leg diameter (labels from C1 to C5) and for bay-variable leg diameter (labels from C6 to C11). The capabilities of the proposed autonomous design approach align with the established objectives, enabling the generation of preliminary designs for various topologies (by varying the number of legs and bracings). In terms of mass efficiency, the most favorable of the obtained designs is the one labeled as C3.

Looking in depth at the lighter solutions that meet the design requirements, Figs. 9 and 10 illustrate the evolution of diameters, thicknesses, cross-sectional area, and Ultimate Limit State (ULS) safety factor for legs and braces (γ_{ULS}) along the entire height of

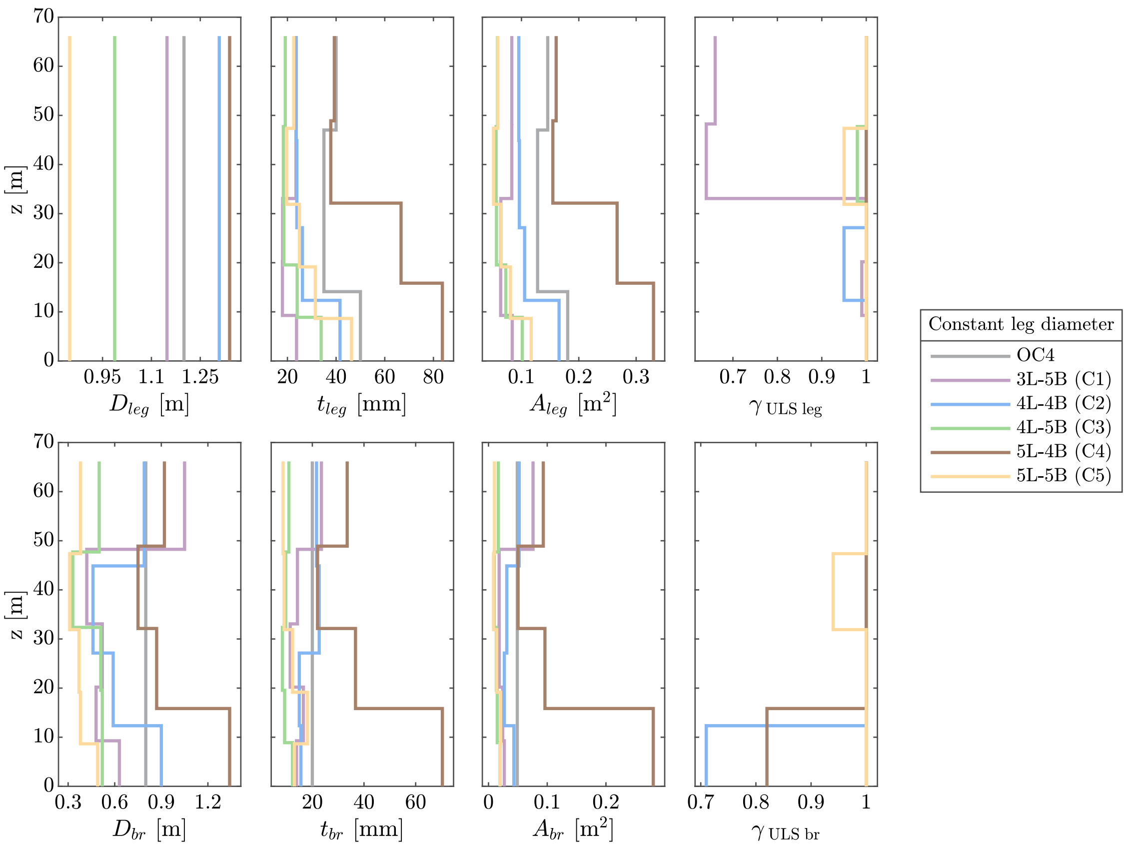

Fig. 9. Diameter (D_{leg} and D_{br}), thickness (t_{leg} and t_{br}), cross-sectional area (A_{leg} and A_{br}) and ULS safety factor of the legs and braces ($\gamma_{\mathrm{ULS\,leg}}$ and $\gamma_{\mathrm{ULS\,br}}$) for the best jackets topologies with constant leg diameters.

the jacket, for both constant (Fig. 9) and bay-variable (Fig. 10) leg diameters, for the best candidates identified by the algorithm, grouped by topology.

Note that in Fig. 9, for the case where the leg diameter remains constant, the changes in the cross-sectional area of the legs are derived from the variations in thickness in each bay section. The highest cross-sectional area along the legs is found at the base of the jacket, where the maximum values of utilization factor ($\gamma_{\mathrm{ULS}} = 1$) are reached. The cross-sectional areas of the bracing bars tend to be higher at the top, in the splash zone where the waves impact, and at the bottom, where there is a significant transfer of stresses between the braces and the legs.

Fig. 10 displays the lightest candidates by geometric configuration for the bay-variable leg diameter. In this case, in almost all jackets the ULS utilization factor along the legs is close to 1. This indicates that allowing the diameter and thickness to present independent values at each bay level results in a better adaptation of the leg geometry to the stress requirements. Similar to the previous case, the braces require a larger cross-sectional area at the top and bottom of the jacket. In comparison, all cases, except for the one with 5 legs and 4 braces for constant leg diameter and 3 legs and 4 braces for variable leg diameter cases, result in a smaller cross-sectional area than that of the reference OC4 jacket in all bay sections.

The autonomous design capability of the algorithm allows additional aspects of the geometry to be analyzed, enabling the structural behavior to be understood. For example, the relation between the jacket mass and the angle of inclination of the braces, β_{br}, or the angle formed by the legs with the vertical (batter angle), α_{leg}, is studied. The angle of inclination of the braces is influenced by the number of braces and by the bottom leg opening. A greater number of braces results in a smaller batter angle of the braces, and vice versa. Similarly, a larger bottom leg opening results in a smaller angle of inclination of the braces, and vice versa. Note that the angle remains constant at each level, therefore, the height of the braces changes with the depth of the jacket in each bay section. Fig. 11 plots the angle of inclination of the braces and the total mass of the jacket for all candidate solutions that meet the design requirements. The number of legs (mark type), braces (mark color) and leg diameter geometry (filled/empty) are represented following the same legend than in Fig. 8. Additionally, the mass of the reference OC4 jacket and its angle of inclination of the braces are represented for reference. The median batter angle of the braces of all jackets represented is 46.08°, which falls within the typical range of 45° to 60° for lattice structures. These angles optimize the amount of material and balance the axial forces, as the bars function as connecting rods that efficiently transmit the loads [46,47]. For design purposes, international standards [48] advise using brace angles between 30° and 60°.

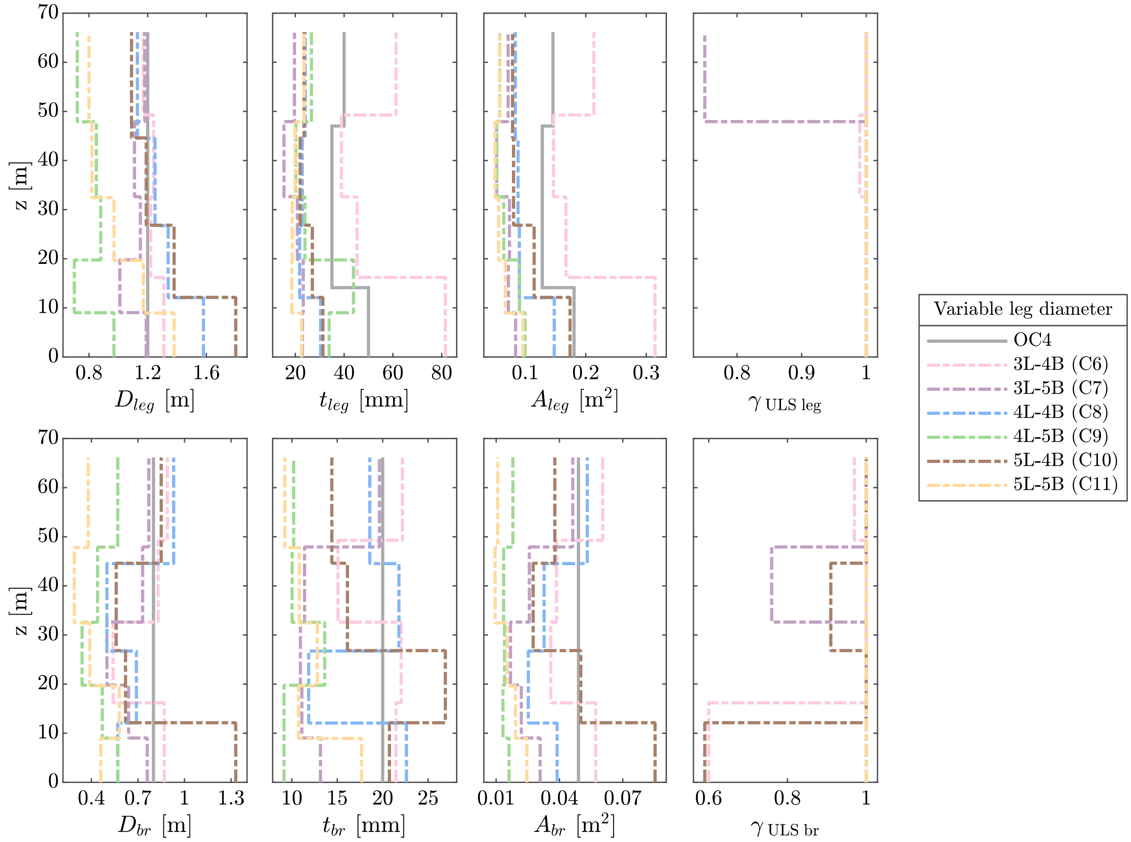

Fig. 10. Diameter (D_{leg} and D_{br}), thickness (t_{leg} and t_{br}), cross-sectional area (A_{leg} and A_{br}) and ULS safety factor of the legs and braces ($\gamma_{\mathrm{ULS\,leg}}$ and $\gamma_{\mathrm{ULS\,br}}$) for the best jackets topologies with variable leg diameters.

Fig. 12 represents the batter angle of the legs and the total mass of the candidate solutions, following the same labeling as in Fig. 11. Designs with a wider lower leg opening have a larger batter angle. This makes jackets lighter than those with a narrower bottom leg opening, as they do not require a larger cross-sectional area because a wider batter angle increases the stability of the assembly, increasing the leg length and improving its load-bearing capacity. Therefore, it is important to find a balance between the batter angle and the total mass of the jacket. The median batter angle for all candidate solutions represented in Fig. 12 is relatively low, 4.20°.

4.3. Eigenmodes analysis

The natural frequencies of the substructure-wind turbine assembly must be between the 1P frequency (rotor rotation) and the 3P frequency (three times the rotor rotation speed) to avoid resonance of the structure.

Fig. 13 shows the fundamental frequency and the mass of candidate solutions meeting the design requirements. The number of legs (mark type), braces (mark color) and leg diameter geometry (filled/empty) are represented following the same legend than in Fig. 8. In addition, the 105% 1P and 95% 3P frequency boundaries are plotted. The fundamental frequencies of all resulting candidate solutions are close to the 3P limit, reflecting a tendency for structures for increasing stiffness. In addition, solutions with fewer braces and legs need to be stiffer, being even closer to the 3P limit. More precisely, average natural frequencies of 0.313 Hz, 0.307 Hz and 0.302 Hz are found for the 3, 4 and 5 legs configurations, respectively. As for the number of bracings, average natural frequencies are found to be 0.322 and 0.301 Hz of 4 and 5 braces configurations, respectively. It can be said that the objective of jacket mass reduction can cause the substructure-OWT assembly to be stiffer. In other words, by considering the optimization of jacket mass the proposed methodology yields solutions that are approaching the limit boundary of 3P. To better understand this, Fig. 14 plots the structural fundamental frequency as a function of the mass of the jacket for the lightest candidate solutions that meet the design requirements. The number of legs (mark type), braces (mark color) and leg diameter geometry (filled/empty) are represented following the same legend than in Fig. 8. As previously mentioned, a decrease in mass generally results in stiffer structures. However, within the set of already optimized best solutions, design plays a significant role that leads to more efficient shapes and better distributed elements in such a way that solutions with less mass tend to be also less rigid.

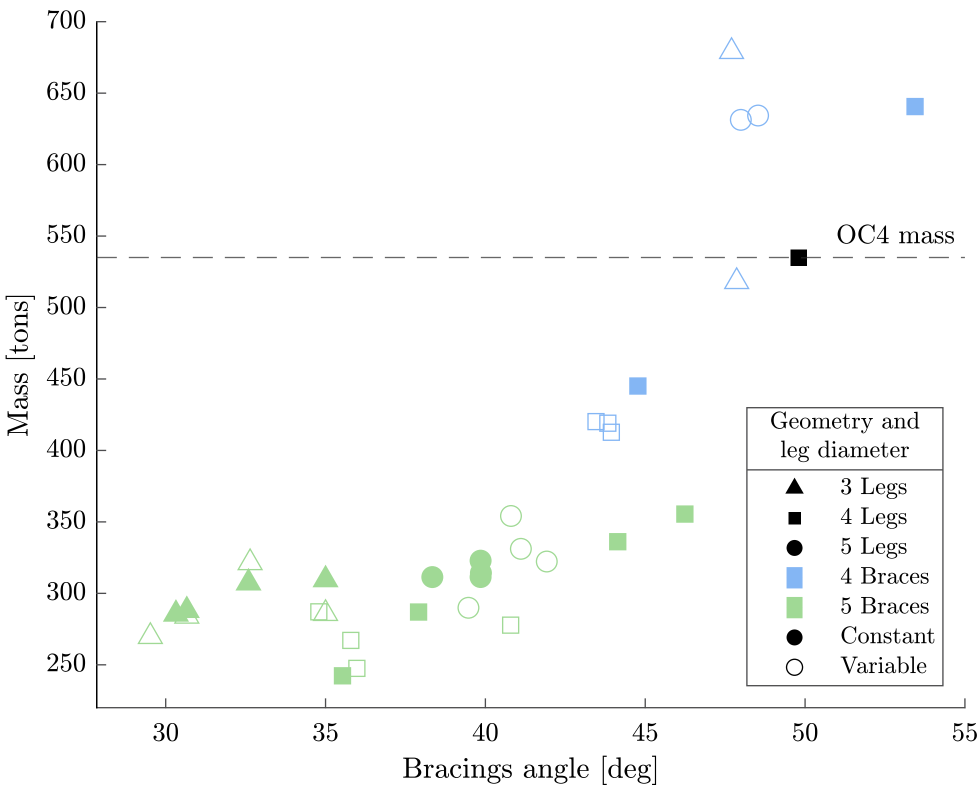

Fig. 11. Comparison between the angle of inclination of the braces and the total mass of the jacket for all candidate solutions that meet the design requirements.

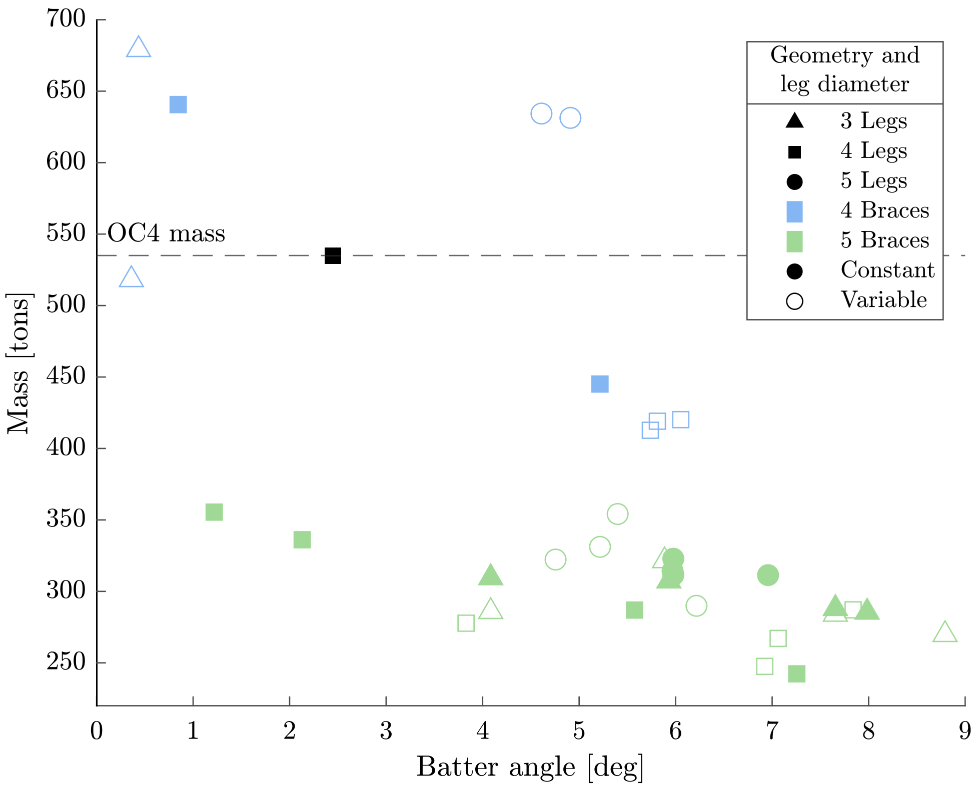

Fig. 12. Comparison between the batter angle and the total mass of the jacket for all candidate solutions that meet the design requirements.

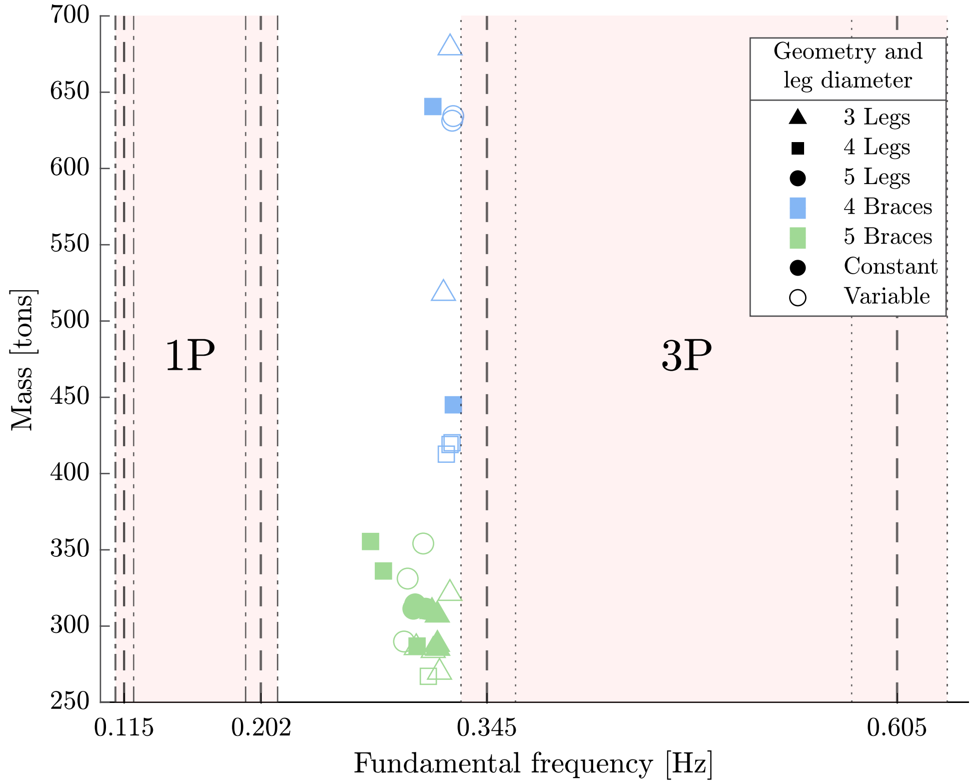

Fig. 13. Fundamental frequency of the candidate solutions that meet the design requirements and the 1P and 3P boundaries.

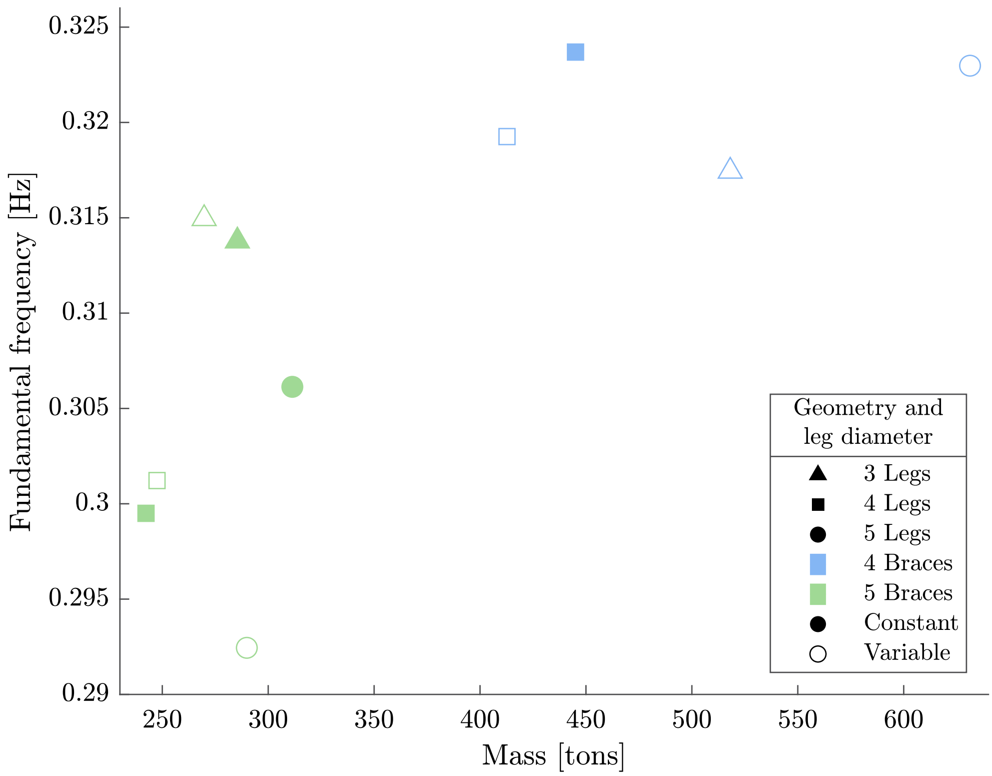

Fig. 14. Fundamental frequency of the lightest candidate solutions as a function of mass of the jacket.

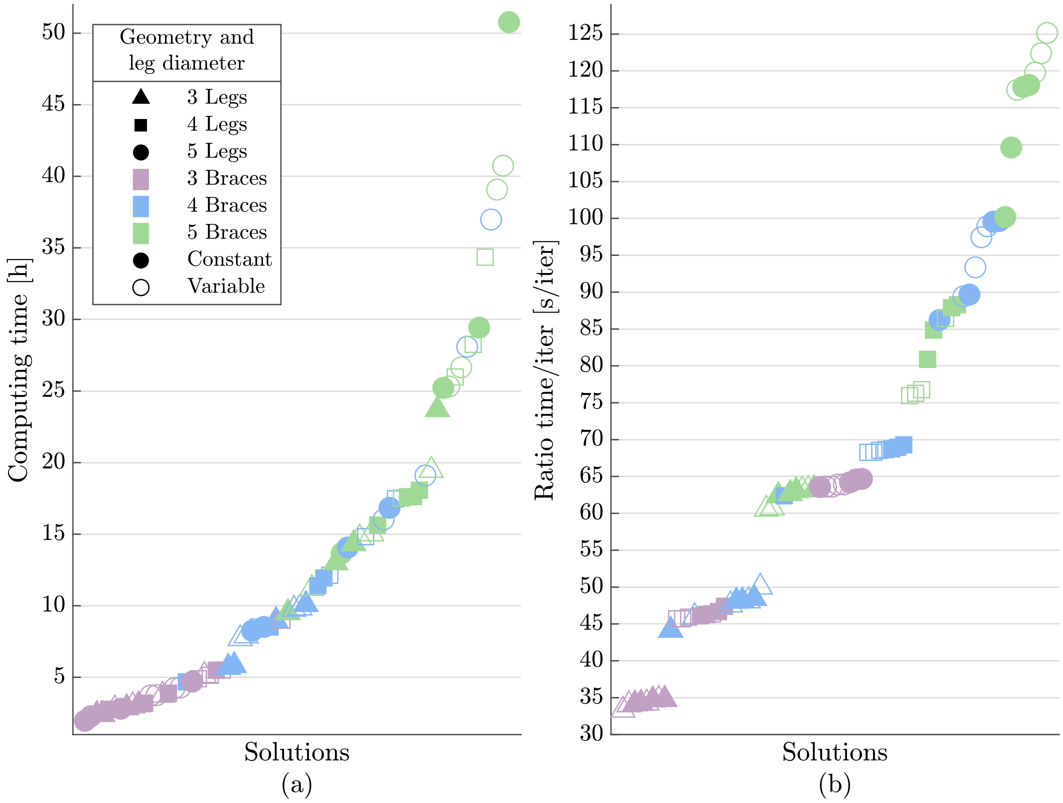

Fig. 15. (a) Total computing time for all the 72 cases. (b) Computing time per iteration for all the 72 cases.

4.4. Computing time

The duration required for the execution of the algorithm depends on various factors. Firstly, the time needed for analyzing and assembling the structure's applied loads, constructing the global stiffness matrix used in the FEM, and solving the system of equations. Other aspects influencing the total analysis time are inherent to the PSO algorithm, like the size of the swarm, the number of iterations utilized or the number of variables. Generally, jackets with fewer legs or braces may require less computation time than those with more intricate geometries and a higher number of variables.

Fig. 15a shows, in ascending order, the calculation time taken for each geometric topology and run of the 72 jackets, whether they meet the verification criteria or not. The execution was carried out by parallelizing 40 process threads in two 32-core Intel(R) Xeon(R) Platinum 8362 CPU at 2.80 GHz, 252 GB RAM computer. The number of legs (mark type), braces (mark color) and leg diameter geometry (filled/empty) are represented following the same legend than in Fig. 8. The number of braces is one of the most computationally demanding factors. The more braces there are, the longer the algorithm will take to execute.

Similar to what is shown in Fig. 15a, Fig. 15b plots the ratio of total time of the swarm, in seconds, per total number of iterations. The number of legs has the same impact on the calculation time as the number of braces. As a result, 3-leg jackets require less execution time than 4 or 5 leg jackets. However, the variable structural sections of the legs in each bay section require longer execution times as the number of legs and braces increases, except for structural topologies with fewer members. It can be seen that the time per iteration is not affected by the constant or bay-variable leg diameter for jackets with 3 legs and braces.

5. Conclusions

This paper proposes a novel strategy for the autonomous design and optimization of jacket support structures for Offshore Wind Turbines. The presented methodology is aimed at generating initial jacket designs of various topologies that meet a set of design requirements and structural verifications, allowing the obtained candidates to be used later in more advanced calculation stages as initial designs. To this end, a cost-efficient framework that involves a Particle Swarm Optimization algorithm coupled to a Finite Element structural Model was proposed. One of the features of this proposal is the use of a precomputed non-random initial population formed by candidate jacket designs that already meet a number of important criteria, as defined by Jalbi and Bhattacharya [24], and that imply a very low computational effort. Therefore, it is worth highlighting the fact that the proposed methodology searches for candidate and optimized designs from scratch, in contrast to other optimization algorithms that require the input of an initial design to be optimized. Another advantage in this regard is that this framework generates not only a single candidate, but a family of candidate designs in each run. Another feature is the use of a two-stages fitness function that allows to search first for feasible structural candidates and, afterwards, for designs optimized by weight that still meet all considered structural requirements in terms of Ultimate and Fatigue Limit States, and of geometric restrictions. The methodology is presented for the design of jackets composed by 3, 4 or 5 legs, with variable or constant structural sections, and any number of bays. The well-known NREL-5MW reference wind turbine, founded on the OC4 reference jacket support structure is considered as a benchmark case.

Upon analyzing the proposed methodology, it is found that:

- The precomputed initial population yields better results than standard random initial swarms, and also makes the whole framework much more robust in terms of increasing the likelihood of finding both feasible and optimized solutions. By quickly and autonomously filtering out the less promising options, the methodology optimizes the time spent in the design phase.
- The proposed two-stages fitness functions help to guide the search process and avoid stagnation. This, together with the precomputed initial population, allows an efficient exploration of the search space.
- The methodology can be easily adapted to different design criteria and environmental conditions, and it is applicable to any type of wind turbine, facilitating the adjustment of initial parameters and constraints to obtain suitable initial designs.
- The methodology allows to quickly identify candidate jackets with various geometric topologies that can serve as preliminary designs. Although structural verifications are not exhaustive at this stage, it is ensured that the selected preliminary designs meet a set of basic structural checks, guaranteeing that the obtained candidates are, at the very least, viable from a general perspective before conducting a more detailed evaluation.

Upon analyzing the results obtained from the study case, it is concluded that:

- The proposed strategy not only finds the OC4 reference jacket substructure, but also many other different and lighter alternatives. More specifically, feasible solutions for all 3, 4 and 5-legged jacket possibilities, and for 4 and 5 bays, are found, with the 4 legs – 5 bays topology being the one with the lowest total mass.
- The optimal batter angle for the jacket legs is found to lie within the 4° to 8° range, with the median of the best solutions in 4.20°, while the optimal batter angle for the bars that form the X-type braces is found to lie within the 35° to 60° range, with the median of the best solutions in 46.08°.
- The fundamental frequencies of most best candidate solutions tend to be as close to the 3P limit as possible, which indicates that stiffer structures tend to be more efficient.

CRediT authorship contribution statement

Borja Benítez-Suárez: Writing – review & editing, Writing – original draft, Visualization, Software, Methodology, Investigation, Formal analysis, Conceptualization. **Román Quevedo-Reina:** Writing – review & editing, Software, Methodology, Conceptualization. **Guillermo M. Álamo:** Writing – review & editing, Writing – original draft, Supervision, Project administration, Methodology, Formal analysis, Conceptualization. **Luis A. Padrón:** Writing – review & editing, Writing – original draft, Project administration, Methodology, Funding acquisition, Formal analysis, Conceptualization.

Declaration of competing interest

The authors declare that they have no known competing financial interests or personal relationships that could have appeared to influence the work reported in this paper.

Acknowledgments

This research has been funded by Ministerio de Ciencia e Innovación and Agencia Estatal de Investigación (MCIN/AEI/10.13039/501100011033) of Spain through research project PID2020-120102RBI00. B. Benítez-Suárez is a recipient of the predoctoral research fellowship (FPI2024010008) from the Consejería de Universidades, Ciencia e Innovación y Cultura and European Social Found Plus (FSE+). Also, R. Quevedo-Reina is a recipient of the FPU research fellowship (FPU19/04170) from the Ministerio de Universidades (MIU) of Spain. This research was partially supported by ACIISI, Spain–Gobierno de Canarias and European ERDF Funds Grant EIS 2021 04.

Data availability

Data will be made available on request.

References

[1] Hille Erik. Europe's energy crisis: Are geopolitical risks in source countries of fossil fuels accelerating the transition to renewable energy? Energy Econ 2023;127:107061.
[2] Joyce Lee, Feng Zhao. GWEC | GLOBAL WIND REPORT 2022. Technical report, Global Wind Energy Council; 2022.
[3] Sánchez Sergio, López-Gutiérrez José-Santos, Negro Vicente, Esteban María Dolores. Foundations in offshore wind farms: Evolution, characteristics and range of use. Analysis of main dimensional parameters in monopile foundations. J Mar Sci Eng 2019;7(12):441.
[4] Damiani Rick, Dykes Katherine, Scott George. A comparison study of offshore wind support structures with monopiles and jackets for US waters. J Phys Conf Ser 2016;753:092003.
[5] Johnston Barry, Foley Aoife, Doran John, Littler Timothy. Levelised cost of energy, a challenge for offshore wind. Renew Energy 2020;160:876–85.
[6] Jiang Zhiyu. Installation of offshore wind turbines: A technical review. Renew Sustain Energy Rev 2021;139:110576.
[7] Jung Christopher, Schindler Dirk. The properties of the global offshore wind turbine fleet. Renew Sustain Energy Rev 2023;186:113667.
[8] Wu Xiaoni, Hu Yu, Li Ye, Yang Jian, Duan Lei, Wang Tongguang, Adcock Thomas, Jiang Zhiyu, Gao Zhen, Lin Zhiliang, Borthwick Alistair, Liao Shijun. Foundations of offshore wind turbines: A review. Renew Sustain Energy Rev 2019;104:379–93.
[9] Chew Kok-Hon, Tai Kang, Ng Eddie Yin Kwee, Muskulus Michael. Optimization of offshore wind turbine support structures using an analytical gradient-based method. Energy Procedia 2015;80:100–7.
[10] Chew Kok-Hon, Tai Kang, Yin Kwee Ng Eddie, Muskulus Michael. Analytical gradient-based optimization of offshore wind turbine substructures under fatigue and extreme loads. Mar Struct 2016;47:23–41.
[11] Oest Jacob, Sandal Kasper, Schafhirt Sebastian, Stieng Lars Einar S, Muskulus Michael. On gradient-based optimization of jacket structures for offshore wind turbines. Wind Energy 2018;21(11):953–67.
[12] Marjan Ali, Huang Luofeng. Topology optimisation of offshore wind turbine jacket foundation for fatigue life and mass reduction. Ocean Eng 2023;289:116228.
[13] Vorpahl Fabian, Popko Wojciech, Kaufer Daniel. Description of a basic model of the UpWind reference jacket for code comparison in the OC4 project under IEA wind annex XXX. Germany: Fraunhofer Institute for Wind Energy and Energy System Technology (IWES); 2011, p. 450.
[14] Jonkman Jason, Butterfield Sandy, Musial Walter, Scott George. Definition of a 5-MW reference wind turbine for offshore system development. 2009.
[15] Sandal Kasper, Verbart Alexander, Stolpe Mathias. Conceptual jacket design by structural optimization. Wind Energy 2018;21(12):1423–34.
[16] Bak Christian, Zahle Frederik, Bitsche Robert, Kim Taeseong, Yde Anders, Henriksen Lars Christian, Hansen Morten Hartvig, Blasques Jose Pedro Albergaria Amaral, Gaunaa Mac, Natarajan Anand. The DTU 10-MW reference wind turbine. In: Danish wind power research 2013. 2013.
[17] Sandal Kasper, Latini Chiara, Zania Varvara, Stolpe Mathias. Integrated optimal design of jackets and foundations. Mar Struct 2018;61:398–418.
[18] Gentils Theo, Wang Lin, Kolios Athanasios. Integrated structural optimisation of offshore wind turbine support structures based on finite element analysis and genetic algorithm. Appl Energy 2017;199:187–204.
[19] Zheng Shunyun, Li Chao, Xiao Yiqing. Efficient optimization design method of jacket structures for offshore wind turbines. Mar Struct 2023;89:103372.
[20] Wang Zhenyu, Mantey Selase Kwame, Zhang Xin. A numerical tool for efficient analysis and optimization of offshore wind turbine jacket substructure considering realistic boundary and loading conditions. Mar Struct 2024;95:103605.
[21] Cruz Rodrigo Oliveira, Duarte Grasiele Regina, de Lima Beatriz Souza Leite Pires, Jacob Breno Pinheiro. Optimization of steel jackets to support offshore wind turbines using evolutionary algorithms. J Offshore Mech Arct Eng 2023;146(2):022001.
[22] Lee Yeon-Seung, González José A, Lee Ji Hyun, Kim Young Il, Park Kwang-chun, Han Soonhung. Structural topology optimization of the transition piece for an offshore wind turbine with jacket foundation. Renew Energy 2016;85:1214–25.
[23] Ali Ahmer, De Risi Raffaele, Sextos Anastasios. Finite element modeling optimization of wind turbine blades from an earthquake engineering perspective. Eng Struct 2020;222:111105.
[24] Jalbi Saleh, Bhattacharya Subhamoy. Concept design of jacket foundations for offshore wind turbines in 10 steps. Soil Dyn Earthq Eng 2020;139:106357.
[25] Jalbi Saleh, Bhattacharya Subhamoy. Closed form solution for the first natural frequency of offshore wind turbine jackets supported on multiple foundations incorporating soil–structure interaction. Soil Dyn Earthq Eng 2018;113:593–613.
[26] Quevedo-Reina Román, Álamo Guillermo M, François Stijn, Lombaert Geert, Aznárez Juan J. Importance of the soil–structure interaction in the optimisation of the jacket designs of offshore wind turbines. Ocean Eng 2024;303:117802.
[27] Arany Laszlo, Bhattacharya Suby, Macdonald John, John Hogan Stephen. Design of monopiles for offshore wind turbines in 10 steps. Soil Dyn Earthq Eng 2017;92:126–52.
[28] Frohboese Peter, Schmuck Christian, Hassan Garrad. Thrust coefficients used for estimation of wake effects for fatigue load calculation. In: European wind energy conference. 2010, p. 1–10.
[29] DNV GL AS. DNVGL-RP-c205: Environmental conditions and environmental loads. 2017.
[30] Morison John R, Johnson Joseph W, Schaaf Samuel A. The force exerted by surface waves on piles. J Pet Technol 1950;2(05):149–54.
[31] DNV GL AS. DNVGL-ST-0437: Loads and site conditions for wind turbines. 2016.
[32] Friedman Zvi, Kosmatka John B. An improved two-node timoshenko beam finite element. Comput Struct 1993;47(3):473–81.
[33] DNV GL AS. DNVGL-RP-C202: Buckling Strength of Shells. 2017.
[34] DNV GL AS. DNVGL-ST-0126: Support structures for wind turbines. 2018.
[35] DNV GL AS. DNVGL-RP-C203: Fatigue design of offshore steel structures. 2016.
[36] Kennedy James, Eberhart Russell. Particle swarm optimization. In: Proceedings of iCNN'95-international conference on neural networks, vol. 4. IEEE; 1995, p. 1942–8.
[37] Eberhart Russ C, Shi Yuhui. Comparing inertia weights and constriction factors in particle swarm optimization. In: Proceedings of the 2000 congress on evolutionary computation. CEC00 (cat. no. 00TH8512), vol. 1. IEEE; 2000, p. 84–8.
[38] The MathWorks Inc. Matlab version: 9.12.0 (r2022a). 2022.
[39] Mezura-Montes Efrén, Coello Carlos A Coello. Constraint-handling in nature-inspired numerical optimization: past, present and future. Swarm Evol Comput 2011;1(4):173–94.
[40] Pedersen Magnus Erik Hvass. Good parameters for particle swarm optimization. Tech. Rep. HL1001, Copenhagen, Denmark: Hvass Lab; 2010, p. 1551–3203.
[41] Vemula Naveen Kumar, De Vries WE, Fischer Tim, Cordle Andrew, Schmidt Björn. Design solution for the upwind reference offshore support structure. 2010.
[42] Tran Thanh-Tuan, Lee Daeyong. Development of jacket substructure systems supporting 3MW offshore wind turbine for deep water sites in South Korea. Int J Naval Archit Ocean Eng 2022;14:100451.
[43] Zhang Puyang, Li Jingyi, Gan Yi, Zhang Jinfu, Qi Xin, Le Conghuan, Ding Hongyan. Bearing capacity and load transfer of brace topological in offshore wind turbine jacket structure. Ocean Eng 2020;199:107037.
[44] Chakrabarti Subrata. Handbook of offshore engineering (2-volume set). Elsevier; 2005.
[45] McClell Bramlette, Reifel Michael D. Planning and design of fixed offshore platforms. Springer US; 1986.
[46] Vasiliev Valery V, Razin Alexander F. Anisogrid composite lattice structures for spacecraft and aircraft applications. In: Fifteenth international conference on composite materials. Compos Struct 2006;76(1):182–9.
[47] Batista Eduardo de Miranda, Vellasco Pedro, de Lima Luciano. Tubular structures XV: Proceedings of the 15th international symposium on tubular structures, Rio de Janeiro, Brazil, 27-29 2015. CRC Press; 2015.
[48] NORSOK Standard. Design of steel structures. N-004, rev, 2. 2004.